Journal of Molecular Structure 1245 (2021) 131077

Contents lists available at ScienceDirect

Journal of Molecular Structure

journal homepage: www.elsevier.com/locate/molstr

Synthesis, characterization, molecular structure, and computational studies on 4(1*H*)-pyran-4-one and its derivatives

Oluwatosin Yemisi Audu[a], Jessica Jooste[a], Frederick P. Malan[a], Olayinka O. Ajani[b], Natasha October[a,*]

[a] Department of Chemistry, University of Pretoria, Lynnwood Road, Hatfield, Pretoria, 0002, South Africa
[b] Department of Chemistry, College of Science and Technology, Covenant University, PMB 1023, Nigeria

ARTICLE INFO

Article history:
Received 12 April 2021
Revised 21 June 2021
Accepted 7 July 2021
Available online 11 July 2021

Keywords:
Computational
Synthesis
Molecular
Characterization
Coupling
4(1*H*)-pyran-4-one

ABSTRACT

4(1*H*)-Pyridone-based compounds have shown promise as potent bioactive inhibitors against a broad range of diseases, particularly malaria. Our interest in 4(1*H*)-pyridones initiated the design and synthesis of a series of 4(1*H*)-pyridone derivatives, with the hope of finding new antimalarial leads. The synthesis of 4(1*H*)-pyran-4-one analogues (4(1*H*)-pyridone intermediates was successfully achieved using palladium catalyzed Suzuki-Miyaura coupling reactions. The synthesized 4(1*H*)-pyran-4-ones were unambiguously confirmed by TGA, ^{13}C, ^{1}H NMR, and IR spectroscopic analysis. Further comprehensive insights to rationalize the outcome of several reactions were deduced by means of single crystal X-ray diffraction, which was used to determine the single crystal structures of compounds **4** and **5**. Compounds **5, 9** and **9a-e** were successfully synthesized in moderate to excellent yields, apart from compound **9e** which gave a very low yield. NMR and XRD analysis of the by-product of compound **9e** showed that the boronic acid substituents reacted with each other in a side-reaction reminiscent to aryl boronic acid homo coupling or Ullmann coupling reactions. Complimentary DFT analysis of the pyranone and pyridone compounds provided insight into the substituent effect of the pyranone compounds with regards to the stability and lack of reactivity to form the corresponding pyridone compounds.

1. Introduction

Pyrones are important class of unsaturated oxygenated six-membered heterocycles that contains a pyran ring, incorporating a ketone functionality at positions 2 or 4 of the pyran ring, (Fig. 1) [1].

Pyrones are used as key intermediates in organic synthesis, owing to the presence of the conjugated dienes and ester moieties, which promote further derivatization to afford highly structurally diverse compound libraries [2–5]. Thus, pyrones are essential building blocks, employed in the preparation of biological active heterocyclic compounds, which amongst others include; 4(1H)-pyridone, α-chymotrypsin, coumarins, pheromones, and solano-pyrones [6–8]. Also, pyrones and derivatives thereof are major composite of natural products and their notable less toxic nature, make them valuable candidates for further drug development [9]. Literature studies particularly highlight the pharmaceutical properties of 2- and -4 pyrone scaffolds as anticancer, [8,10] antimalarial, [11] antimicrobial, [12,13] antidiabetics [14,15] anti-Alzheimer agents [7], (Fig. 2).

To further explore the medicinal potential and to take advantage of the versatile handle offered by the pyrone scaffold, a defined series of 4(1*H*)-pyran-4-one-based derivatives were designed and synthesized. Thus, synthesis of the series of the 2,6-dimethyl-3-(4-substituted-phenyl)-4*H*-pyran-4-one, **9a-e** (Fig. 3) were successfully achieved, when aromatic substituents were linked together *via* palladium catalyzed Suzuki-Miyaura [16] coupling and was further investigated. [17]

2. Results and discussion

The synthetic pathway in Scheme 1 was employed to prepare the precursor, 3-(4-bromophenyl)-2,6-dimethyl-4*H*-pyran-4-one 4 [2,16,17]. Synthesis of the methyl aryl ketone, 1-(4-bromophenyl)propan-2-one **3**, was achieved *via* reductive methylation of 4-bromophenylacetic acid in good yield (72 %), using 1-

* Corresponding author.
E-mail address: natasha.october@up.ac.za (N. October).

https://doi.org/10.1016/j.molstruc.2021.131077
0022-2860/

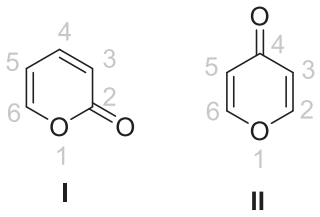

Fig. 1. Structures of 2-pyrone (**I**) and 4-pyrone (**II**)

methylimidazole as the catalyst. Compound **3** was confirmed with ^{1}H NMR, which revealed the disappearance of the signal related to the acetic acid OH group, as well as formation of the methyl substituent, which resonate upfield as 3H at 2.14 ppm. Thus, the cyclization of 1-(4-bromophenyl) propan-2-one **3** with acetic anhydride in the presence of Eaton's reagent, [$(PO_2)_2O$] [CH_3SO_2OH], resulted in the formation of 3-(4-bromophenyl)-2,6-dimethyl-4*H*-pyran-4-one **4** in a moderate yield (48 %). The formation of **4** was further established by means of ^{1}H NMR and single-crystal X-ray diffractometry (SCXRD). Cyclization of **3** leading to the formation of **4** was confirmed with the appearance of a vinylic proton, which resonate downfield as a singlet at 6.22 ppm while two sharp singlets of the two –CH_3 groups on position 2 and 6 on the 4(1*H*)-pyranone ring were seen upfield at 2.15 and 2.28 ppm respectively. Interestingly, extensive analysis of the crystalline products in the product mixture leading to the isolation and identification of compound **4** allowed for the identification of compound **5**, which was identified by means of SCXRD. The detection of this compound could further explain the observed low yield of **4** by the relative increased reactivity of **4**.

Single crystals of **4** and **5** suitable for X-ray diffraction were grown from saturated Hexane:Ethyl acetate(3:1) solutions (Fig. 4). Crystals of **4** crystallized in the monoclinic $P2_1/c$ space group with Z = 4, whereas crystals of **5** crystallized in the orthorhombic space group $P2_12_12_1$ also with Z = 4. A slight bend of the 4-BrPh group connected to the pyridone ring structure in **4** is seen with a O14-C3-C4-C7 torsion angle of -5.1(5)° (Tables S1 and S2, SI). The corresponding angle in **5** is a near-linear 2.0(12)° with the remaining 4-BrPh group only slightly twisted (O14-C3-C2-C17 = -7.0(12)°). Each of the arene groups twist with respect to the pyridine ring with torsion angles of C3-C4-C7-C8 = 49.1(5)° (4), C3-C4-C7-C8 = -67.9(11)° (5), and C3-C2-C17-C18 = 119.7(8)° (5). Molecules in the structure of **4** packs in three dimensions as a ribbon with the pyridone moieties of adjacent molecules linking by weak intramolecular forces, and then overlays with the arene rings to other adjacent molecules (Figure S1, SI). A similar pattern is also seen with the packing of molecules in the structure of **5**, except that adjacent molecules is connected *via* the weak intramolecular forces from adjacent arene rings on either side of each molecule (Figure S2, SI). No other mentionable hydrogen bonding or pi-pi stacking interactions were observed in either of the structures of **4** or **5**. Typical bond distances and angles are observed in **4** and **5** compares well with each other as well as with other closely related structures [18].

Subsequently, using two different types of boronic acids, bis(pinacolato)diboron **7** and **7′** (Scheme 2) and 2-substituted phenylboronic acids, compounds **8a-f**, were used to prepare analogues of 4*H*-pyran-4-one *via* Suzuki-Miyaura coupling reactions using 10 mol% of either $PdCl_2$(dppf) or $PdCl_2(PPh_3)_2$ as catalyst. In the reaction forming **8a**, 4-bromostilbene was coupled with bis(pinacolato)diboron **7**, using $PdCl_2$(dppf) as catalyst along with potassium acetate, to give the compound 4,4,5,5-tetramethyl-2-(4-phenethylphenyl)-1,3,2-dioxaborolane **8a** in moderate yield (62 %). The ^{1}H NMR of **8a** revealed 12 protons of the four –CH_3 groups with a sharp intense singlet seen upfield at 1.28 ppm. Compound **4** in turn coupled with compound **8a** in the presence of $PdCl_2(PPh_3)_2$ (10 mol%) and potassium carbonate to give the compound 2,6-dimethyl-3-{4′-[(1*E*)-2-phenylethenyl]-[1,1′-biphenyl]-4-yl}-4*H*-pyran-4-one **9a** in a moderate yield (39 %). The ^{1}H NMR spectrum of **9a** displayed additional four aromatic proton signals, namely 7.24, 7.26, 7.58, and 7.60 ppm, which shifted downfield, confirming the formation of compound **9a**.

Following the success of the reaction producing compound **9a** from **8a**, the series of compounds 2-substituted phenylboronic acids **8b-f** were also employed as coupling partners in the Suzuki-Miyaura reaction with compound **4** in the presence of $PdCl_2(PPh_3)_2$ (10 mol%) and K_2CO_3 to give moderate to good yields of the corresponding adducts **9b-e** (39 – 75 %) (Scheme 2).

The series of compounds **9a-e** were successfully synthesized, however although **9f** was synthesized**,** the yield was not determined due to its decomposition on standing, which led to the formation of undesired crystallized products. Upon closer inspection

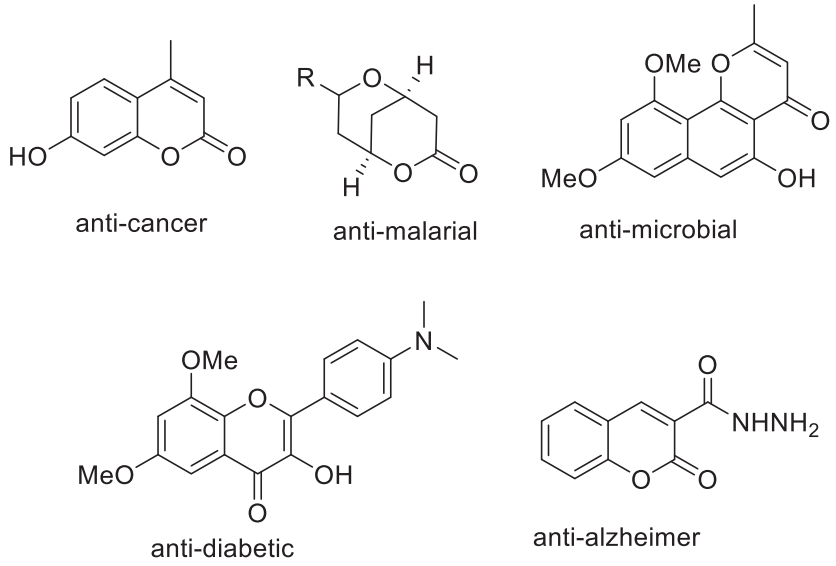

Fig. 2. Structures of some pyrones that displayed biological activities [8], [11],[13],[15],[7].

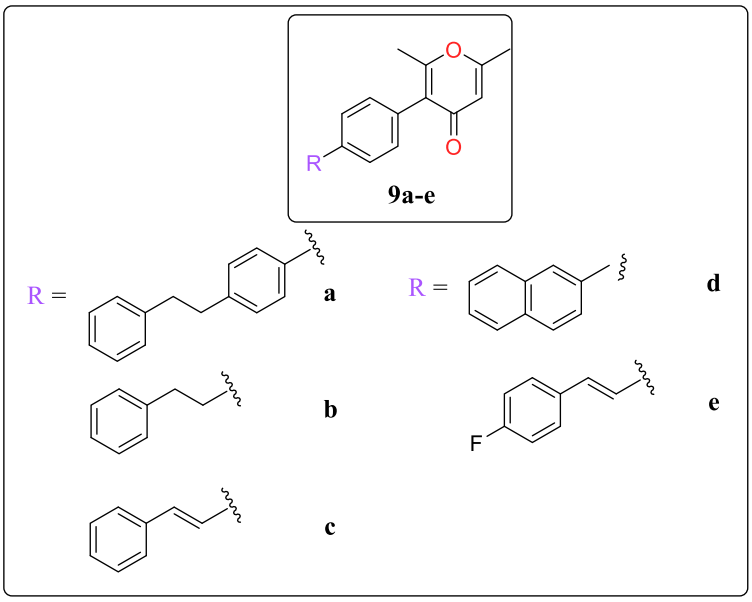

Fig. 3. Series of synthesized 2,6-dimethyl-3-(4-substitutedphenyl)-4*H*-pyran-4-ones, **9a-e**

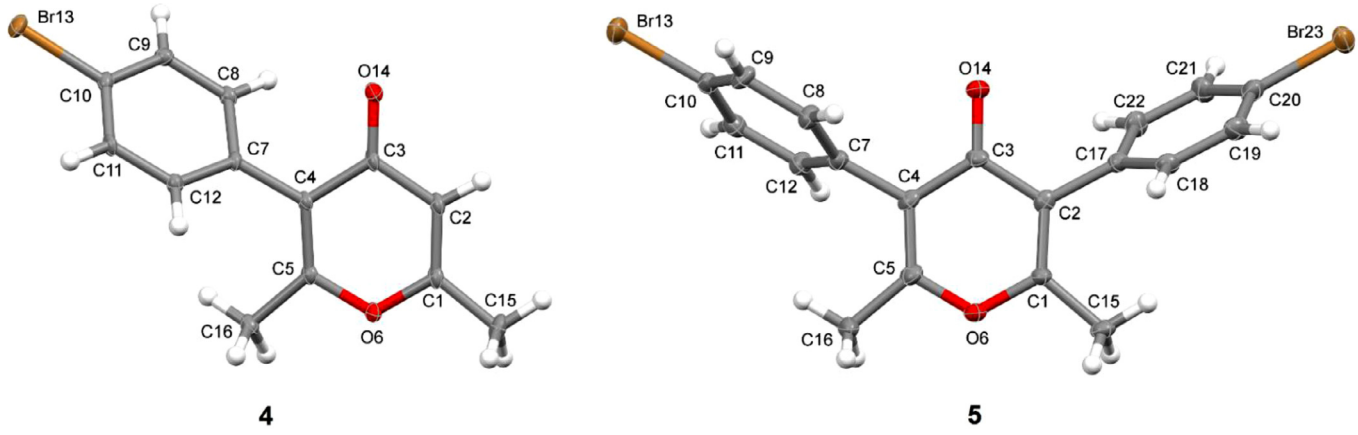

Fig. 4. Crystal structures of Compounds **4** and **5**

of the product mixture of **9d** and the decomposed product **9f**, a single crystal picked from each mixture, analyzed using SCXRD, revealed the presence of a corresponding by-product of compound **9d** and crystalline product **9f** (**9d'** and **9f'** respectively, Figures S3 and S4, SI). This may resulted from the homocoupling of the boronic acid substituents which has been observed before in related Suzuki-Miyaura or Ullmann coupling reactions [19]. The formation of these by-products may be suppressed or even avoided in the case where the aryl boronic acid is added portion wise to the reaction mixture, or should the use of a protected boronic acid be possible, be used to avoid homocoupling. Using compound **9c** as a spectroscopy study, **9c** displayed 18 protons in its ^{1}H NMR spectrum. Four aromatic protons were seen as multiplets between 7.62-7.50 ppm: two aromatic protons were observed at 7.5-7.4 ppm while the remaining two aromatic protons were noticed at 7.3-7.2 ppm. The two alkene (H-C=C-H) protons were observed as a singlet at 7.16 ppm. A singlet proton of a vinyl of the 4*H*-pyran-4-one ring was also observed downfield at 6.26 ppm while the remaining two $-CH_3$ protons at the position 2 and 6 of the 4*H*-pyran-4-one ring were observed downfield TMS at 2.3 and 2.2 ppm, respectively. The result of the ^{13}C NMR of **9c** presented twenty-one carbon atoms with 15 peaks, with the δ_C value ranging from 178.5 ppm to 18.7 ppm. A carbonyl carbon substituent on the position 4 of the 4*H*-pyran-4-one is seen at 178.5 ppm while other twelve carbon atoms are aromatic carbons, displayed around 164.8 ppm to 113.8 ppm and the remaining two carbon atoms are ascribed to two $-CH_3$ groups at the position 2 and 6 of the 4*H*-pyran-4-one ring, seen at 18.7 and 19.8 ppm respectively.

Attempts to synthesize the targeted 4(1*H*)-pyridone moieties **10a-e** unfortunately was unsuccessful. The unsuccessful synthesis of the target compounds **10a-e** could be due to the initial introduction of electron donating group in the substituted phenylboronic acids **8a-f**, which led to reduction in the reactivity of the pyrone ring. This alternatively could have also led to unfavourable S_N2 nucleophilic substitution of amino group on position 1 of the 4(1*H*)-pyran-4-one ring. Steric hindrance present in the 4(1*H*)-pyran-4-one ring structure may also been a contributing factor towards the unsuccess of the final aminolation reaction, which could in turn resulted in an increase in the activation energy required for the reaction to proceed, and ultimately lowered the overall observed

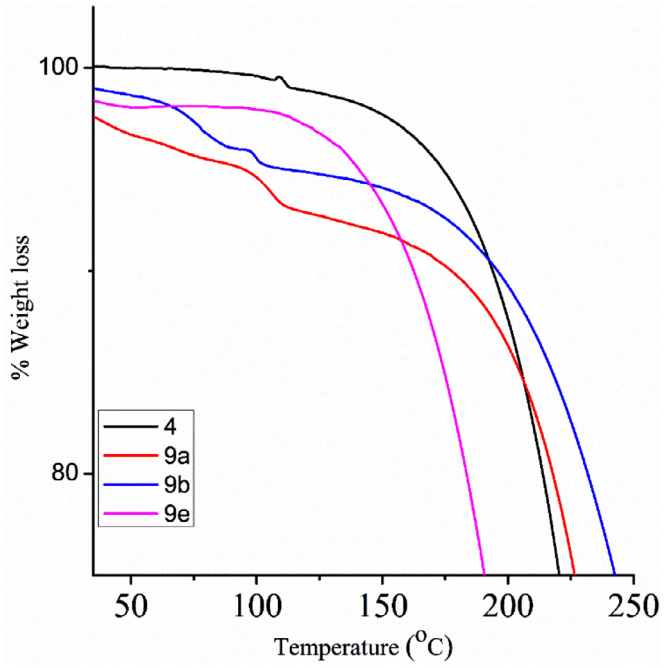

Fig. 5. Thermogravimetric Analysis (TGA) of Selected Compounds **4, 9a, 9b** and **9e**.

rate of reaction [20]. The intermediates **9a-e** could not be considered for antimalarial testing, since the presence of the NH group in corresponding compounds **10a-e** have demonstrated imperative for antimalarial activity.

As a result of to lack of reactivity displayed by the 4(1*H*)-pyran-4-ones and since the conversion of 4-pyrones to 4-pyridones requires high temperatures, the thermal properties of 4*H*-pyran-4-ones **4, 9a, 9b**, and **9e** were analyzed using the thermogravimetric analysis (TGA,Fig. 5) [21]. The TGA displayed a high rate of thermal decomposition and instability of these compounds, even at temperature of 37 °C, 73 °C, and 104 °C respectively, lower than the temperature (140 °C) [22] at which the reaction would have taken place using ammonium hydroxide (NH_4OH) as the reactant [22]. Compound **4** (precursor to compounds **9a-e**) was observed to be quite stable as compared to **9a, 9b**, and **9e** as seen in Fig. 5.

2.1. DFT analysis

In order to gain more insight into the substituent effect(s) of the boron-containing compounds on the (by-)product formation, as well as the lack of reactivity of compounds **9a-e** to form **10a-e**, a Density Functional Theory (DFT) computation study was performed. In general, input structures were obtained from the crystallographic information files (CIFs) for the relevant compounds (or derivations thereof) and were further optimized in the gas phase until conversion with zero imaginary frequencies. Considering the C-C coupled compounds **9a-e**, their corresponding frontier molecular orbitals and associated properties may be analyzed to help explain the difference in stability, as well as their lack of reactivity with NH_4OH to form the corresponding compounds **10a-e**. The highest occupied molecular orbital (HOMO) may be visualized as providing the source of electrons in an oxidizing reaction and therefore be correlated to the ionization potential of the compound. In contrast, the lowest unoccupied molecular orbital (LUMO) may, in turn, be visualized as the electron sink in a reduction reaction and hence be correlated to the electron affinity of the compound. The HOMOs and LUMOs of compounds **9a** and corresponding **10a** (theoretical), as well as **9c** and corresponding **10c** (theoretical) were selected as representative examples and are shown in Fig. 6. In general, the HOMOs of compounds **9a-e** are distributed mainly over the biphenyl group (at the site where C-C coupling took place). In the case of aliphatic linkers (e.g. **9a**), electron diffusion *via* resonance is inhibited, whereas the compounds containing unsaturated linkers (e.g. **9c**), electron diffusion to include the remainder of arene groups is present. The LUMOs of both examples are comparable with one another, where the LUMOs are delocalized mainly over the biphenyl groups as well as the pyranone ring structure (Fig. 6. As part of the general Baeyer pyridine synthesis mechanism, [23] it is accepted that the first step toward pyridone formation would be the nucleophilic attack of the ammonia molecule at a partially electron-poor carbon atom adjacent to the oxygen atom (Scheme 3). In this particular case, electron transfer between both the ether-like oxygen (in the pyranone ring), and the carbonyl oxygen is important to help form an anionic oxygen intermediate specie in the pyranone ring moiety. In general, the LUMO of the reactant, and the HOMO of the corresponding product molecule should correlate in the sense that electron transfer could be visualized. Collectively, the reactivity (reduction/oxidation) of the series of compounds of **9** is suggested to lie within the biphenyl moiety, and only slightly populated within the pyrone ring system (containing the oxygen-containing functional groups) where electron transfer is anticipated. It is therefore interesting to note that the corresponding HOMO of the product molecules (series of compounds **10**) is again only slightly populated on either of the two oxygen atoms and more so on the biphenyl moiety. Collectively this may hint towards the lack of reactivity of the series of compounds of **9** with nucleophiles such as NH_3 to form the corresponding compounds **10**. The interpretation and conclusion with regards to reactivity does not change after inclusion of the implicit solvent model (EtOH), in an attempt to more closely mimic the reaction conditions. For example, upon full optimization of compound **9a** (including the implicit solvent model of EtOH), the HOMO and LUMO is practically indistinguishable from **9a** (gas phase optimized).

The energy gap (ΔE, energy difference between the HOMO and LUMO) of each compound may directly be compared to provide information on their respective molecular reactivity and stability. A molecule with a small energy gap is therefore considered to be more polarizable, softer, more reactive and kinetically less stable. The energy gap (ΔE), ionization potential (I), electron affinity (A), electronegativity (χ), chemical potential (μ), chemical hardness (η), chemical softness (S), and electrophilicity index (ω) of compounds **9ae** and **10a-e** are included in Table 1. From the data it is apparent that the energy gap of the pyranone-based compounds (**9a-e**) generally is slightly larger than the energy gap of the corresponding pyridone compounds (**10a-e**), suggesting higher stability and hence lowered reactivity. Inclusion of solvent effect (EtOH as implicit solvent model) further increases both ΔE and the ionization potential slightly by *ca.* 0.02 and 0.1 eV respectively, suggesting lower reactivity compared to the corresponding isolated molecule in the gas state. Comparing the effect of the functional groups in **9a-e**, the energy gap varies between 3.91 and 5.17 eV, where the C_2H_2-linked (ethene bridge) functional groups (**9c** and **9e**) are the least stable (3.91 and 3.94 eV, respectively), and the C_2H_4-linked (ethylene bridge) functional groups (**9a** and **9b**) are the most stable (4.55 and 5.17 eV, respectively). This trend is also reflected in their corresponding electron affinity (A), chemical softness (S) and electrophilicity indices (ω), where compounds having the lowest electron affinity would be the compounds most likely to act as Lewis acids in the reactions converting pyranones to pyridones. The remainder of the computed reactivity descriptors compare relatively well among the two series of compounds (**9a-e** and **10a-e**) as well as functional-group related compounds between the two series of compounds.

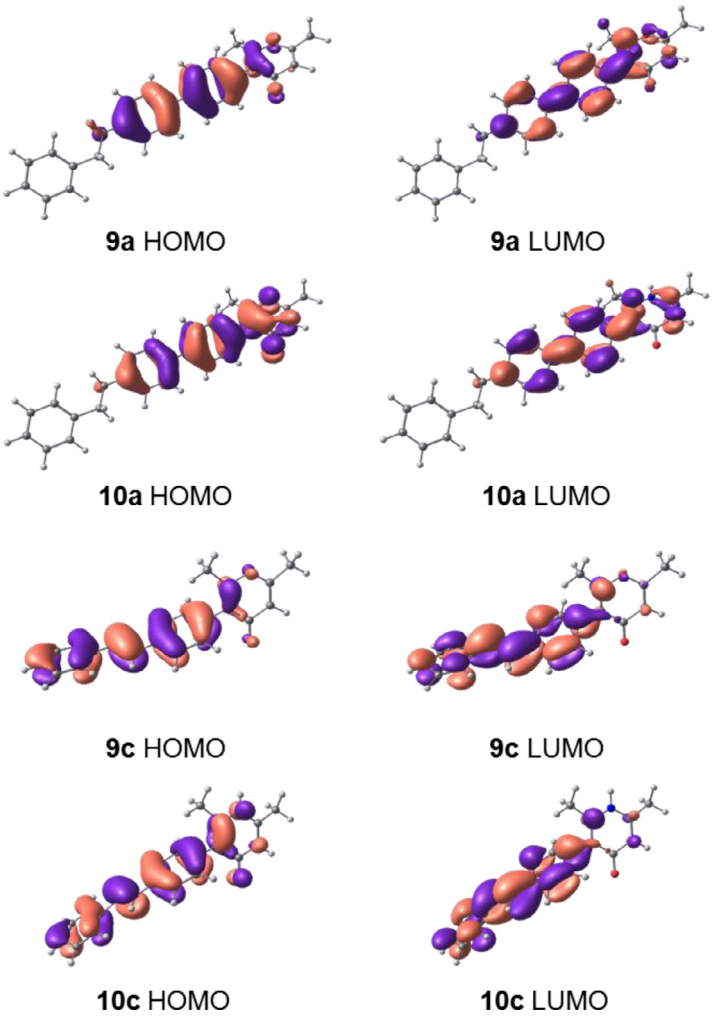

Fig. 6. B3LYP functional DFT calculated HOMOs and LUMOs of the indicated neutral compounds from this study. A contour of 0.03 e/Å^3 was used for the MO plots.

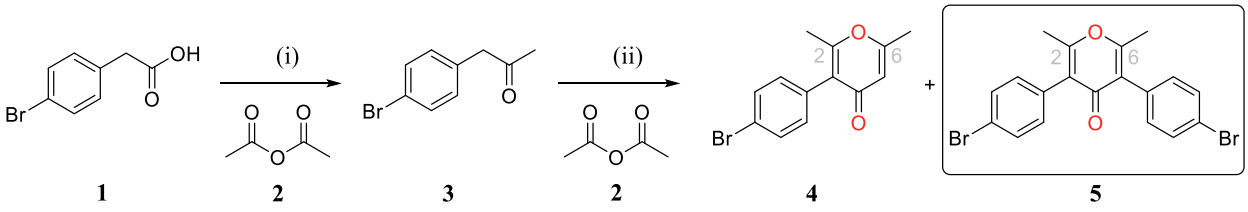

Scheme 1. Synthesis of compounds **3**-**5**. Reagents and conditions: (i) 1-Methylimidazole, rt, N_2, 15 h; (ii) Eaton's reagent, 95°C, 2 h.

Table 1
Molecular parameters and reactivity descriptors of compounds **9a-f** and **10a-f**.

Parameter	Compound											
	9a	9b	9c	9d	9e	9f	10a	10b	10c	10d	10e	10f
Energy gap[a] (ΔE) (eV)	4.55	5.17	3.91	4.42	3.94	4.08	4.44	5.09	3.95	4.37	3.88	4.05
Ionization potential[b] (I) (eV)	5.84	6.23	5.63	5.82	5.67	5.63	5.60	5.78	5.46	5.68	5.46	5.46
Electron affinity[c] (A) (eV)	1.29	1.06	1.72	1.41	1.73	1.55	1.16	0.69	1.51	1.31	1.58	1.41
Chemical potential[d] (μ) (eV)	-3.56	-3.64	-3.68	-3.61	-3.70	-3.59	-3.38	-3.23	-3.49	-3.50	-3.52	-3.44
Electronegativity[e] (χ) (eV)	3.56	3.64	3.68	3.61	3.70	3.59	3.38	3.23	3.49	3.50	3.52	3.44
Chemical hardness[f] (η) (eV)	4.55	5.17	3.91	4.42	3.94	4.08	4.44	5.09	3.95	4.37	3.88	4.05
Chemical softness[g] (S) (eV)	0.22	0.19	0.26	0.23	0.25	0.25	0.23	0.20	0.25	0.23	0.26	0.25
Electrophilicity index[h] (ω) (eV)	1.39	1.28	1.73	1.48	1.74	1.58	1.28	1.03	1.54	1.40	1.60	1.46

[a] $\Delta E = E_{HOMO} - E_{LUMO}$. [b] $I = -E_{HOMO}$. [c] $A = -E_{LUMO}$. [d] $\mu = -(I + A)/2$. [e] $\chi = -\mu$. [f] $\eta = I - A$. [g] $S = 1/\eta$. [h] $\omega = \mu^2/2\eta$.

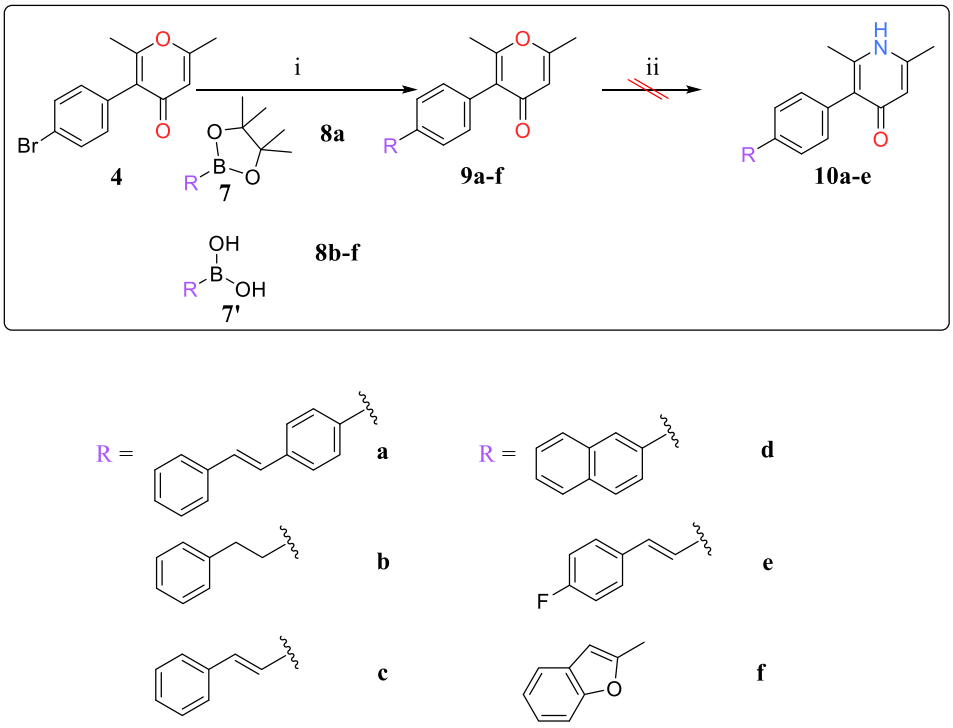

Scheme 2. Synthesis of targets **9a-f** *via* boronic acids and **10a-e** *via* ammonium hydroxide. Reagents and conditions: (i) $PdCl_2(PPh_3)_2$, K_2CO_3, distilled H_2O, 80 °C, 3 h; (ii) NH_4OH, EtOH, 150 °C, 50 h. In the case of **9a** the dioxaborolane **8a** is reacted instead of the boronic acid.

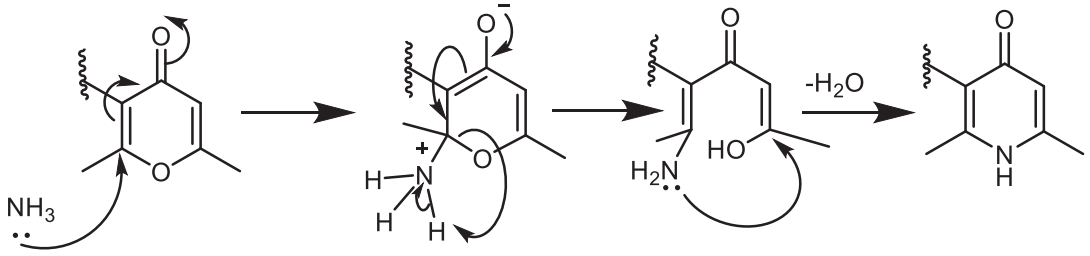

Scheme 3. Nucleophillic substitution mechanism for the conversion of 4-pyrone to 4-pyridone

3. Conclusion

In conclusion, new derivatives of 2,6-dimethyl-4*H*-pyran-4-one compounds **5** and **9a-e** was successfully synthesized using palladium catalyzed Suzuki-Miyaura coupling reactions. Single crystal structures of compounds **4** and **5** were determined using X-ray diffraction and revealed their unique identities upon which the side reactions were identified. Compounds **5** and **9a-e** were successfully synthesized with moderate to good yields apart from compound **9f** which yield was not determined due to its decomposition. SCXRD analysis of the by-products of the reactions forming compound **9d** (**9d'**) and decomposed material **9f** (**9f'**) showed that the homocoupling of boronic acids remain to be one of the major side-reactions occurring that lower the yield of the main products. DFT analysis showed that electron density in the HOMO of compounds **9a-e** is mainly distributed over the substituted R-groups (resulting biphenyl moiety after C-C coupling) and hence, suggests a lack of reactivity *via* either of the oxygen-atoms in the pyranone ring. TGA analysis confirmed the high rate of instability and thermal decomposition of the selected 2,6-dimethyl-4*H*-pyran-4-one compounds **9a, 9b,** and **9e**, and as result we were unable to synthesize the target compounds **10a-e.**

4. Experimental

All reagents used for the purpose of this research were purchased commercially from Sigma-Aldrich Chemicals (South Africa). All solvents were purchased from Merck Chemicals South Africa. Solvents such as DMF used were dried accordingly before usage. DMF was distilled under nitrogen into 4A molecular sieve beads from calcium hydride at 60 °C and kept overnight. During solvent extraction, organic fractions collected were dried using anhydrous magnesium sulfate $MgSO_4$ or sodium sulfate Na_2SO_4 respectively. Solvents were evaporated under reduced pressure, using IKRV 10 Rotary evaporator. Merck silica gel (0.063-0.200 mm) was used for Column chromatography, while Thin Layer Chromatography TLC, was done using Merck 60 F254 pre-coated silica gel plates and were further visualized under ultraviolet light at 254 nm. Melting points were determined with the aid of Gallenkamp melting point, in an open capillary tube and are uncorrected. The ^1H NMR and ^{13}C NMR spectra were collected on a Bruker Avance 400 (at 400.21 MHz for ^1H and 100.64 MHz for ^{13}C) spectrometer by the means of $CDCl_3$, CH_3OD or DMSO-d_6, depending on the solubility of each compound. The chemical shifts were reported in part per million ppm relative to tetremethylsilane, (TMS) as an internal standard.

4.1. Procedure for the synthesis of 1-(4-bromophenyl)propan-2-one 3

A solution of 4-bromophenolacetic acid (10.01 g, 46.83 mmol, 1.0 eq.) in acetic anhydride anhydride (21.5 mL, 227.87 mmol, 4.9 eq.) was stirred and purged at room temperature for 10 min under inert conditions. To the mixture was added 1-methylimidazole (1.80ml, 22.73 mmol, 0.49 eq.) which initiated the reaction. The mixture stirred for 16 hours at ambient temperature. The reaction was quenched by the addition of distilled water (30ml) to the reaction flask after which TLC indicated complete conversion of starting materials into product. The mixture was extracted with ethylacetate (200 mL), and washed with saturated $NaHCO_3$ (3 × 100 ml). The organic layer was dried (Mg_2SO_4), evaporated to dryness *in vacuo* to afford crude product that was purified *via* flash column chromatography, eluting with Hex:EtAOc (8:2). The combined fractions were evaporated to dryness to obtain **3** as a canary yellow solid, in excellent yields.

Yield: 7.15 g, 72.19 % MP:247-249 °C; FT-IR: νmax (neat)/cm^{-1} 3085, 2962, 2843, 2808, 2726, 2666, 2509, 1671, 1578, 1421, 1272, 751. ^{1}H NMR (300 MHz, DMSO-d_6) δ_H 7.49 (d, $^3J_{HH}$ = 8.4, $^3J_{HBr}$ = 6.0 Hz, 2H, Ar*H*), 7.14 (d, $^3J_{HH}$ = 8.4, $^3J_{HBr}$ = 5.5 Hz, 2H, Ar*H*), 3.78 (s, 2H, CH_2), 2.14 (s, 3H, CH_3) ^{13}C NMR (101 MHz, $CDCl_3$) δ_C 178.2, 164.8, 162.6, 131.9, 131.6, 125.7, 122.1, 113.8, 19.8, 18.6.

Synthesis of 3-(4-bromophenyl)-2,6-dimethyl-4H-pyran-4-one, 4: Eaton's reagent (22.86 mL, 145.5mmol, 4.41 eq.) was added to acetic anhydride (11.1 mL, 116.4 mmol, 5.98 eq.) in a 2-neck round bottom flask at room temperature. The mixture was allowed stir before being heated to 95 °C under argon. To this solution was added 4-bromophenylacetone (7.0 g, 32,9 mmol, 1 eq.) drop-wise and the reacting mixture refluxed for 2 hrs, after which TLC indicated complete consumption of starting materials. The reacting mixture was allowed to cool to room temperature, poured into an ice-water bath (50 mL) and extracted with toluene (5 × 250 mL), washed with saturated $NaHCO_3$ (2 × 300 mL). The organic layer was dried (Mg_2SO_4) and concentrated *in vacuo* to afford the crude product as a brown solid that was purified by flash column chromatography, eluting with Hex:EtOAc (3:1). Yield: 4.36 g, 47.5 %; MP: 105.9-110.4 °C; FT-IR: νmax (neat)/cm^{-1} 3062, 3034, 2922, 2853,1658, 1610, 1395, 1234, 1068, 967, 838. ^{1}H NMR (400 MHz, $CDCl_3$) δ_H 7.55 (dd, $^3J_{HH}$ = 11.2, $^3J_{HBr}$ = 6.4 Hz 2H, Ar*H*), 7.12 (dd, $^3J_{HH}$ = 10.8, $^3J_{HBr}$ = 6.0 Hz 2H, Ar*H*), 6.21 (s, 1H, C=C*H*), 2.30 (s, 3H, CH_3), 2.19 (s, 3H, CH_3). ^{13}C NMR (101 MHz, $CDCl_3$) δ_C 178.2, 164.8, 162.6, 131.9 (2C), 131.6 (2C), 131.5, 125.7, 122.1, 113.8, 19.8, 18.6.

4.2. Procedure for the synthesis of 4,4,5,5-tetramethyl-2-(4-styrylphenyl)-1,3,2-dioxaborolane 8a

A solution of 4-bromostilbene (518.5 mg, 2.00 mmol, 1 eq.) in dry 1,4-dioxane under an inert atmosphere was stirred at ambient temperature and charged with bis(pinacolate)diboron (661 mg, 2.60 mmol, 1.3 eq.), $PdCl_2$(dppf) (163.2 mg, 0.2 mmol, 0.1 eq.), and KOAc (589.1 mg, 6.00 mmol, 3 eq.) in succession. The reaction mixture was heated at 120 °C for 5 h, after which TLC indicated complete conversion of starting materials into products. The solution was cooled to room temperature, diluted with EtOAc and filtered through celite. The filtrate was washed with water (2 × 200 mL) and brine (2 × 200 mL), dried ($MgSO_4$) and evaporated under reduced pressure and the crude product was purified *via* column chromatography with Hex:EtOAc (9:1) to afford **8a** as a white powder. Yield: 0.382 g, 62.4 %; MP: 116-120°C; FT-IR: νmax (neat)/cm^{-1} 2978, 2973, 2923, 2854, 1602, 1354, 1142, 963, 858. ^{1}H NMR (400 MHz, $CDCl_3$) δ_H 7.72 (d, $^3J_{HH}$ = 8.1 Hz, 2H, Ar*H*), 7.48 – 7.41 (m, 4H, Ar*H*), 7.29 (t, $^3J_{HH,HH}$ = 8.0 Hz, 2H, Ar*H*), 7.19 (m, 1H, Ar*H*), 7.07(dd, $^3J_{HH}$ =28.4, $^3J_{HH}$ = 16.4 Hz, 2H, *HC*=C*H*), 1.28 (s, 12H,CH_3 × 4).^{13}C NMR (75 MHz, $CDCl_3$) δ_C 140.0(2C), 137.2(2C), 135.1, 129.6(2C), 128.7(2C), 127.8(2C), 126.6(2C), 125.8, 83.8(2C), 24.9(4C).

4.3. General procedure for the synthesis of 2,6-dimethyl-3-phenyl-4(1H)-pyran-4-one derivatives 9a-f

(1*H*)3-(4-Bromophenyl)-2,6-dimethyl-4(1*H*)-pyran-4-one **4** (200 mg, 1.0 eq.), $PdCl_2(PPh_3)_2$ (0.1 eq.), K_2CO_3 (3.0 eq.) were added in succession to a solution of either 4,4,5,5-tetramethyl-2-(4-styrylphenyl)-1,3,2-dioxaborolane **8a** or substituted boronic acids **8b-f** (1.3 eq.**)** in a 1,4-dioxane-water mixture (6 mL, 2:1) under nitrogen gas and stirred at room temperature. The reaction mixture was refluxed (80 °C) for 3 h, after which TLC indicated the reactants had converted to products. The mixture was cooled to ambient temperature, filtered and concentrated *in vacuo*. The resulting residue was taken up in ethyl acetate (20 mL) and washed with water (20 mL). The organic layer separated, and the aqueous layer was extracted with ethyl acetate (50 mL). The combined organic fractions were dried ($MgSO_4$) and concentrated *in vacuo* to afford compounds and the product was purified using prepatory TLC with DCM: Hexane (7:3, v:v) to afford **9a-e** in average to good yields as white to yellow solids.

4(1*H*)4-((*E*)-1,2-Diphenylethene2,6-dimethyl-3-phenyl-4(1*H*)-pyran-4-one, 9a: Compound **8a** (as opposed to the boronic acids) was employed. Yield, 0.010 g, 39%; MP, 260.9 - 262.0°C; FT-IR: νmax (neat)/cm^{-1} 2952, 2921, 2855, 1700, 1319. ^{1}H NMR (400 MHz, $CDCl_3$) δ_H 7.61 – 7.56 (m, 2H, Ar*H*), 7.55 – 7.51 (m, 4H, Ar*H*), 7.47 (d, $^3J_{HH}$ = 7.2 Hz, 2H, Ar*H*), 7.30 (t, $^3J_{HH}$ = 7.6 Hz, 2H, Ar*H*), 7.27 – 7.20 (m, 3H, Ar*H*), 7.09 (s, 2H, *H*-C=C-*H*) 6.17 (s, 1H, -C=C-*H*), 2.23 (s, 3H, CH_3), 2.18 (s, 3H, CH_3). ^{13}C NMR (101 MHz, $CDCl_3$) δ_C 178.6 164.7, 162.7, 140.1, 140.0, 137.3, 136.5, 131.7, 130.6, 128.8, 128.7(2C), 128.2, 127.7, 127.4(2C), 126.9(2C), 126.9, 126.6(2C), 22.7, 18.8.

2,6-dimethyl-3-(4-phenethenylphenyl)-4*H*-pyran-4-one, 9b: Compound **8b** was employed. Yield, 0.13 g, 59 %; MP, 185.3 - 186.8 °C; FT-IR: νmax (neat)/cm^{-1} 3035, 2923, 2853, 1659, 1608, 1407; ^{1}H NMR (400 MHz, $CDCl_3$) δ_H 7.46 (dd, $^3J_{HH}$ = 6.4, $^3J_{HH}$ = 4.0 Hz, 1H), 7.18 (m, 5H, Ar*H*), 7.05 (dd, $^3J_{HH}$ = 14.4, $^3J_{HH}$ = 8.0 Hz, 3H, Ar*H*) 6.16 (s, 1H, C=C*H*), 2.86 (s, 4H, H_2C-CH_2), 2.22 (s, 3H, CH_3), 2.11(s, 3H, CH_3). ^{13}C NMR (101 MHz, $CDCl_3$) δ 178.8, 164.6, 162.7, 141.8, 141.4, 131.9, 131.6, 130.1(2C), 128.5(2C), 128.4(2C), 128.4(2C), 125.9, 113.7, 37.8, 29.7, 19.9, 18.7.

2,6-dimethyl-3-(4-styrylphenyl)-4H-pyran-4-one, 9c: Compound **8c** was employed. Yield, 0.127 g, 55 %; MP: 185.3 - 186.8 °C; FT-IR: νmax (neat)/cm-1 3036, 2922, 2852, 1658, 1608, 1402. ^{1}H NMR (400 MHz, $CDCl_3$) δ_H 7.57 (dd, $^3J_{HH}$ = 12.8, 7.7 Hz, 4H, Ar*H*), 7.39 (t, $^3J_{HH}$ = 7.6 Hz, 1H, Ar*H*), 7.33 – 7.22 (m, 3H, Ar*H*), 7.15 (s, 2H, *HC*=C*H*), 6.26 (s, 1H, C=C*H*), 2.32 (s, 3H, CH_3), 2.24 (s, 3H, CH_3). ^{13}C NMR (101 MHz, $CDCl_3$) δ_C 178.5, 164.6, 162.6, 137.2, 136.9, 131.8, 130.5(2C), 129.0, 128.7(2C), 128.3, 127.7, 126.7(2C), 126.5(2C), 126.3, 113.8, 19.8, 18.7.

2,6-dimethyl-3-[4-(naphthalen-2-yl)phenyl]-4H-pyran-4-one, 9d: Compound **8d** was employed. Yield, 0.44 g, 75.4%; MP: 260.9 - 262.0°C. FT-IR: νmax (neat)/cm^{-1} 3042, 2922, 2852, 1657, 1605, 1406δ_H 7.98 (s, 1H, Ar*H*), 7.81 (dt, $^3J_{HH}$ = 9.0, $^3J_{HH}$ = 5.2 Hz, 3H, Ar*H*), 7.69 (d, $^3J_{HH}$ = 8.3 Hz, 3H, Ar*H*), 7.47 – 7.36 (m, 2H, Ar*H*), 7.28 (d, $^3J_{HH}$ = 8.3 Hz, 2H, Ar*H*), 6.16 (s, 1H, C=C*H*), 2.21 (s, 3H, CH_3), 2.17 (s, 3H, CH_3). ^{13}C NMR (101 MHz, $CDCl_3$) δ_C 178.6, 164.6,162.7, 140.6, 138.2, 133.7, 132.7, 131.7, 130.7(2C), 128.5, 128.2, 127.7, 127.4(2C), 126.30(2C), 125.9, 125.8, 125.6, 113.8, 19.8, 18.8.

3-{4-[(1*E*)-2-(4-fluorophenyl)ethenyl]phenyl}2,6-dimethyl-4*H*-pyran-4-one, 9e: Compound **8e** was employed. Yield, 0.52 g, 54.7%; MP: 175.1 - 175.9; FT-IR: νmax (neat)/cm-1 3040, 2923, 2852, 1650, 1604, 1402; ^{1}H NMR (300 MHz, CDCl3) δ_H 7.60 – 7.45 (m, 4H, Ar*H*), 7.29 – 7.23 (dd, $^3J_{HH}$ =11.2, $^3J_{HH}$ = 5.2 Hz, 2H, *HC*=C*H*), 7.13 – 7.03 (m, 4H, Ar*H*), 6.23 (s, 1H, C=C*H*), 2.31 (s, 3H,

CH_3), 2.24 (s, 3H, CH_3). ^{13}C NMR (75 MHz, $CDCl_3$) δ_C 178.5, 164.6, 163.9, 162.6, 160.7, 136.7, 133.5, 133.4, 131.9, 130.5, 128.1, 127.9, 127.8, 126.4, 126.3, 115.8, 115.5, 113.8, 113.8, 19.7, 18.7.

4.4. X-ray crystallography

Single crystals of **4** and **5** were analysed on a Rigaku XtaLAB Synergy R diffractometer, with a rotating-anode X-ray source (monochromated Cu Kα radiation (k = 1.54184 Å)) and a HyPix CCD detector. Data reduction and absorption were carried out using the CrysAlisPro (version 1.171.40.39a) software package [24]. Empirical absorption correction was performed using spherical harmonics, implemented in SCALE3 ABSPACK scaling algorithm. All X-ray diffraction measurements were performed at 150(1) K, using an Oxford Cryogenics Cryostat. All structures were solved by direct methods with SHELXT-2016 [24] using the SHELXL-2016 [25] algorithm. All H atoms were placed in geometrically idealized positions and constrained to ride on their parent atoms. For data collection and refinement parameters, see the SI (**Tables S1** and **S2**). The X-ray crystallographic coordinates for all structures have been deposited at the Cambridge Crystallographic Data Centre (CCDC), with deposition numbers CCDC 2069544–2069545. The data can be obtained free of charge from The Cambridge Crystallographic Data Centre *via* www.ccdc.cam.ac.uk/data_request/cif.

5. Computational chemistry

All calculations were carried out using Density Functional Theory (DFT) using the B3LYP-D3 (B3LYP with the Grimme empirical dispersion correction D3) hybrid functional [26] [27], as implemented in the ORCA program package (version 4.0.1.2) [28]. The triple-ζ basis set def2-TZVPP [29] and def2-J [30] auxiliary basis set were used for all atoms (B, C, H, N, O, F). The geometries of all compounds were fully optimized without any symmetry restrictions, ensuring that the local minima had zero imaginary vibrational frequencies and to provide the thermal correction to free energies at 298.15 K and 1 atm. Selected calculations were repeated to consider the solvent effect of EtOH, and therefore a conductor-like polarizable continuum model (CPCM) [31] was employed.

Authors' contribution

Oluwatosin Yemisi Audu: Conceptualization, methodology, investigation, data curation and, writing-original draft; **Jessica Jooste**: Investigation; **Frederick P. Malan**: Software, data curation, validation, writing - review and editing, and supervision; **Olayinka O. Ajani**: validation, writing - review and editing; **Natasha October**: Conceptualization, validation, writing - review and editing, and supervision.

Declaration of Competing Interest

The authors declare that they have no known competing financial interests or personal relationships that could have appeared to influence the work reported in this paper.

Acknowledgements

We are grateful to TWAS-NRF South Africa with UID grant no 105464 and Chemistry Department, University of Pretoria.

Supplementary materials

Supplementary material associated with this article can be found, in the online version, at doi:10.1016/j.molstruc.2021.131077.

References

[1] T. Maier, C.A.B. Rodrigues, N. Maulide, Synthesis of c -pyrones via decarboxylative condensation of b -ketoacids, 2016, doi:10.1007/s00706-016-1851-2.
[2] J.S. Lee, Recent Advances in the Synthesis of 2-Pyrones, (2015) 1581–1620. https://doi.org/10.3390/md13031581.
[3] J.C. De Rosa, D. Beatriz, J.M. Fiandor, T. Fraile, M. Garc, E. Herreros, Synthesis, Structure – Activity Relationships of the Novel Antimalarials 5 – Pyridinyl-4(1 H), Pyridones 4 (2018), doi:10.1021/acs.jmedchem.7b01256.
[4] S.A. Usachev, B.I. Usachev, V.Y. Sosnovskikh, Synthesis of 6-hydroxy-5, 6-dihydro-2-pyrones and -pyridones by reaction of 4-aryl-6-trifluoromethyl-2-pyrones with water, hydrazine, and hydroxylamine, 53 (2017) 1294–1301. https://doi.org/10.1007/s10593-018-2209-y.
[5] D.L. Obydennov, L.R. Khammatova, O.S. Eltsov, V.Y. Sosnovskikh, A chemo- and regiocontrolled approach to bipyrazoles and pyridones via the reaction of ethyl 5-acyl-4-pyrone-2-carboxylates with hydrazines, Org. Biomol. Chem. 16 (2018) 1692–1707, doi:10.1039/C7OB02725G.
[6] D.L. Obydennov, L.R. Khammatova, O.S. Eltsov, V.Y. Sosnovskikh, Biomolecular Chemistry bipyrazoles and pyridones via the reaction of ethyl, (2018) 1692–1707. https://doi.org/10.1039/c7ob02725g.
[7] S.K. Yusufzai, M.S. Khan, O. Sulaiman, H. Osman, D.N. Lamjin, Molecular docking studies of coumarin hybrids as potential acetylcholinesterase, butyrylcholinesterase, monoamine oxidase A/B and β-amyloid inhibitors for Alzheimer's disease, Chem. Cent. J. 12 (2018) 128, doi:10.1186/s13065-018-0497-z.
[8] T.F. Schäberle, Biosynthesis of α -pyrones, (2016) 571–588. https://doi.org/10.3762/bjoc.12.56.
[9] S. Berto, E. Alladio, P.G. Daniele, E. Laurenti, A. Bono, C. Sgarlata, G. Valora, R. Cappai, J.I. Lachowicz, V.M. Nurchi, Oxovanadium (IV) Coordination Compounds with Kojic Acid Derivatives in Aqueous Solution, (n.d.) 1–18.
[10] V.D. Reddy, D. Dayal, D.J. Szalda, S.C. Cosenza, M.V.R. Reddy, Ruthenium carbonyl containing 4-pyrones as potent anti-cancer agents, J. Organomet. Chem. 872 (2018) 135–143 https://doi.org/https://doi.org/10.1016/j.jorganchem.2018.04.014.
[11] Y. Liu, L.H. Rakotondraibe, P.J. Brodie, J.D. Wiley, M.B. Cassera, J.S. Miller, F. Ratovoson, E. Rakotobe, V.E. Rasamison, D.G.I. Kingston, Antimalarial 5,6-Dihydro-α-pyrones from Cryptocarya rigidifolia: Related Bicyclic Tetrahydro-α-Pyrones Are Artifacts1, J. Nat. Prod. 78 (2015) 1330–1338, doi:10.1021/acs.jnatprod.5b00187.
[12] G. Obi, J.C. Chukwujekwu, F.R. van Heerden, Synthesis and antimicrobial activity of new prenylated 2-pyrone derivatives, Synth. Commun. 50 (2020) 726–734, doi:10.1080/00397911.2020.1718710.
[13] Y. He, J. Tian, X. Chen, W. Sun, H. Zhu, Q. Li, L. Lei, G. Yao, Y. Xue, J. Wang, H. Li, Y. Zhang, Fungal naphtho-γ-pyrones: Potent antibiotics for drug-resistant microbial pathogens, Sci. Rep. 6 (2016) 24291, doi:10.1038/srep24291.
[14] M.N. Sarian, Q.U. Ahmed, S.Z. Mat So'ad, A.M. Alhassan, S. Murugesu, V. Perumal, S.N.A. Syed Mohamad, A. Khatib, J. Latip, Antioxidant and Antidiabetic Effects of Flavonoids: A Structure-Activity Relationship Based Study, Biomed Res. Int. 8386065 (2017) 2017, doi:10.1155/2017/8386065.
[15] Y. Nayak, V. Hillemane, V.K. Daroji, B.S. Jayashree, M.K. Unnikrishnan, Antidiabetic Activity of Benzopyrone Analogues in Nicotinamide-Streptozotocin Induced Type 2 Diabetes in Rats, Sci. World J. 854267 (2014) 2014, doi:10.1155/2014/854267.
[16] A.A.C. Braga, G. Ujaque, F. Maseras, Mechanism of Palladium-Catalyzed Cross-Coupling Reactions, Comput. Model. Homog. Enzym. Catal. A Knowledge-Base Des. Effic. Catal. (2008) 109–130, doi:10.1002/9783527621965.ch5.
[17] C. Len, S. Bruniaux, F. Delbecq, V.S. Parmar, Palladium-catalyzed Suzuki–Miyaura cross-coupling in continuous flow, Catalysts 7 (2017) 1–23, doi:10.3390/catal7050146.
[18] Mitsuhiro Yonehara, 83 (2011) 2563–2575. https://doi.org/10.3987/COM-11-12352.
[19] C. Arylations, X.A.F. Cook, A. De Gombert, J. Mcknight, L.R.E. Pantaine, M.C. Willis, The 2-Pyridyl Problem : Challenging Nucleophiles in Angewandte Reviews, 2020, pp. 2–26, doi:10.1002/anie.202010631.
[20] B. Pinter, T. Fievez, F.M. Bickelhaupt, P. Geerlings, F. De Proft, On the origin of the steric effect, Phys. Chem. Chem. Phys. 14 (2012) 9846–9854, doi:10.1039/c2cp41090g.
[21] R.A. Adigun, F.P. Malan, M.O. Balogun, N. October, Substitutional effects on the reactivity and thermal stability of dihydropyrimidinone s, J. Mol. Struct. 1223 (2021) 129193, doi:10.1016/j.molstruc.2020.129193.
[22] J.M. Bueno, P. Manzano, M.C. Garc??a, J. Chicharro, M. Puente, M. Lorenzo, A. Garc??a, S. Ferrer, R.M. G??mez, M.T. Fraile, J.L. Lavandera, J.M. Fiandor, J. Vidal, E. Herreros, D. Gargallo-Viola, Potent antimalarial 4-pyridones with improved physico-chemical properties, Bioorganic Med. Chem. Lett. 21 (2011) 5214–5218, doi:10.1016/j.bmcl.2011.07.044.
[23] L. Hintermann, Comprehensive Organic Name Reactions and Reagents. By Zerong Wang., Angew. Chemie Int. Ed. 49 (2010) 2659–2660. https://doi.org/https://doi.org/10.1002/anie.201000292.
[24] Rigaku Oxford Diffraction, CrysAlisPro Software system (2018).
[25] G.M. Sheldrick, Crystal structure refinement with SHELXL, Acta Crystallogr. Sect. C Struct. Chem 71 (2015) 3–8.
[26] A.D. Becke, Density-functional thermochemistry. III. The role of exact exchange, J. Chem. Phys. 98 (1993) 5648–5652, doi:10.1063/1.464913.
[27] C. Lee, W. Yang, R.G. Parr, Development of the Colle-Salvetti correlation-energy formula into a functional of the electron density, Phys. Rev. B. 37 (1988) 785–789, doi:10.1103/PhysRevB.37.785.

[28] M.J. Frisch, G.W. Trucks, H.B. Schlegel, G.E. Scuseria, M.A. Robb, J.R. Cheeseman, G. Scalmani, V. Barone, B. Mennucci, G.A. Petersson, GAUSSIAN 09, Rev. C. 01, D. 01. Wallingford CT: Gaussian, (2010).
[29] F. Weigend, R. Ahlrichs, Balanced basis sets of split valence{,} triple zeta valence and quadruple zeta valence quality for H to Rn: Design and assessment of accuracy, Phys. Chem. Chem. Phys. 7 (2005) 3297–3305, doi:10.1039/B508541A.
[30] F. Weigend, Accurate Coulomb-fitting basis sets for H to Rn, Phys. Chem. Chem. Phys. 8 (2006) 1057–1065, doi:10.1039/B515623H.
[31] M. Cossi, N. Rega, G. Scalmani, V. Barone, Energies, structures, and electronic properties of molecules in solution with the C-PCM solvation model, J. Comput. Chem. 24 (2003) 669–681, doi:10.1002/jcc.10189.